



ELSEVIER

Available online at www.sciencedirect.com

SCIENCE @ DIRECT®

Journal of volcanology
and geothermal research

Journal of Volcanology and Geothermal Research 132 (2004) 31–43

www.elsevier.com/locate/jvolgeores

Porosity and permeability in volcanic rocks: a case study on the Serie Tobífera, South Patagonia, Argentina

P. Sruoga^a, N. Rubinstein^{b,*}, G. Hinterwimmer^c

^a CONICET, SEGEMAR, Av. Julio Roca 651, Piso 10, C.P. 1322 Buenos Aires, Argentina

^b CONICET, Universidad de Buenos Aires, Departamento de Geología, Pabellón 2, Ciudad Universitaria, C.P. 1428 Buenos Aires, Argentina

^c CHEVRON San Jorge S.A., Suipacha 925, C.P. 1322 Buenos Aires, Argentina

Received 26 February 2002; accepted 1 December 2003

Abstract

The Middle to Late Jurassic Serie Tobífera belongs to the Chon-Aike Province and extends all over Patagonia and the Antarctic Peninsula. It consists largely of ignimbrites, epiclastics and rhyolitic lavas and was considered only a minor reservoir rock for oil with fracture permeability. Petrographic and petrophysical data in selected core samples from the Austral Basin were collected to determine the processes controlling the porosity and permeability of these volcanic rocks. The sequence of processes occurring during cooling and in the post-cooling stages can modify, sometimes substantially, their original petrophysic characteristics. The results show that the highest porosity and permeability occur in rocks with quench fractured glasses and in non-welded ignimbrites with gas-pipe structures, followed by autobrecciated rhyolites. Welded ignimbrites, massive glasses and fresh rhyolites have the lowest permeabilities. The new data indicate that tectonic fracturing is not as significant as was considered before and application of these concepts are relevant in the assesment of volcanic reservoir quality.

© 2003 Elsevier B.V. All rights reserved.

Keywords: Tobífera; South Patagonia; volcanics; porosity; permeability

1. Introduction

The ‘Serie Tobífera’ is an informal subsoil name in the Austral Basin. Traditionally, this thick volcanic sequence was envisaged as a secondary reservoir target for oil and gas exploration because of its apparently random reservoir condition. The overlying Springhill sandstone is the main productive reservoir of this basin, although

some oil and gas fields extend into the Serie Tobífera’.

The reservoir characteristics of the Serie Tobífera were rarely studied and simple assumptions were postulated to explain its petrophysics: tectonic fracturing and/or tuff weathering. However, detailed geological and petrophysic studies are needed in order to determine the processes controlling the porosity and permeability in these volcanic rocks.

The aim of this paper is to establish the processes that occur after ignimbritic flows and rhyolitic lavas are emplaced and completely cooled

* Corresponding author.

E-mail address: nora@gl.fcen.uba.ar (N. Rubinstein).

and their effects in modifying the original porosity and permeability. An integrated study of petrographic and petrophysic data in selected core samples from the Austral Basin was carried out in order to assess those processes.

2. Geological setting

The ‘Serie Tobífera’ is a widespread lithostratigraphic unit known as the Chon-Aike Province (Kay et al., 1989) (Fig. 1). It forms a silicic Large Igneous Province (Pankhurst et al., 1998), extending over an estimated area of 1.7×10^6 km² including the Continental Platform. Middle to Late Jurassic in age, this long-lived and widespread volcanism took place in Patagonia along the western margin of Gondwanaland. Many low sulfidation gold and silver deposits are associated with this magmatic event in the Deseado Massif (Schalamuck et al., 1999).

Older radiometric studies (Cazeneuve, 1965) have shown this unit to be of Middle Jurassic

age (160.7 Ma). Only recently SHRIMP U–Pb zircon dating (Pankhurst et al., 2000) allowed defining of three main episodes: V1 (188–178 Ma), V2 (172–162 Ma) and V3 (157–153 Ma). The volcanic activity, which extended over a time span of 35 my, experienced a westward migration reflecting tectonic changes during the different stages of Gondwana break-up (Storey et al., 1992).

The emplacement of this huge volcanic unit was coeval with a regional lithospheric extension regime active since Triassic times. Seismic data indicate that the silicic magmatism is closely related to the initial extensional faulting. The rift system is composed of inverse oriented hemigrabens, controlled by NW–SE trending main faults (Ramos, 1996). The rifting tectonics prevailed until Early Cretaceous times and ultimately led to the opening of the Atlantic ocean. In the early stages of Gondwana break-up a dominantly mafic to bimodal volcanism, probably related to the activity of the Karroo plume, took place (Pankhurst et al., 2000). Subsequently, the volcanic activity became essentially silicic and shifted episodically towards

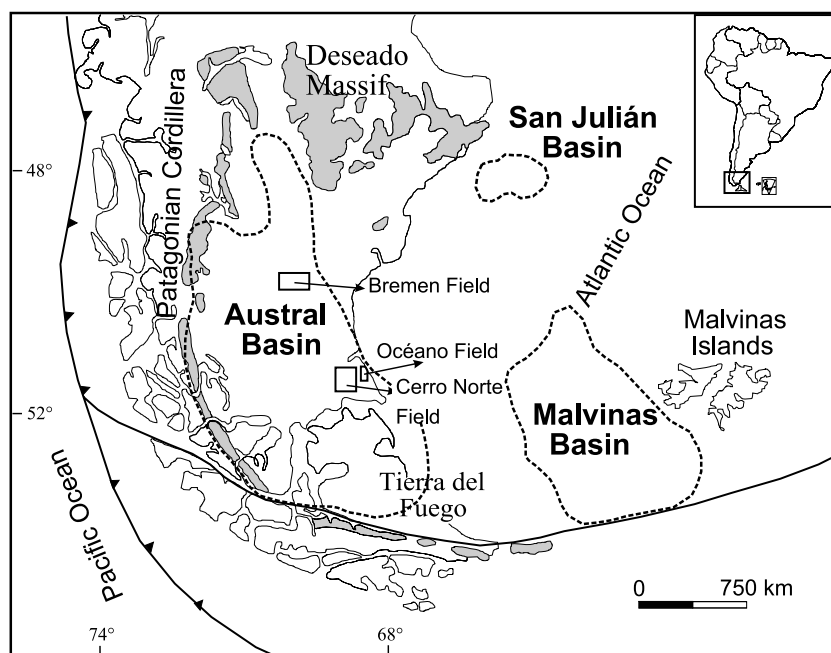


Fig. 1. Sketch map of South Patagonia showing the main outcrop areas of South Chon-Aike Province, the locations of the main oil and gas productive basins and the area of study are shown.

the Pacific margin (Storey et al., 1992). The youngest episode corresponds to the emplacement of the volcanic rocks belonging to the El Quemado Complex and the Ibañez Formation. Geochemical evidence indicates an arc signature for these rocks (Sruoga, 1994) suggesting that after a long period of quasi-static state an increase of the convergence velocity and the development of a magmatic arc took place at this latitude by the end of Cretaceous times. During the Tertiary orogenic cycle, the rift system was reactivated with tectonic inversion along the main fault zones.

Remarkably homogeneous in composition (Sruoga, 1989; Pankhurst et al., 1998), the South Chon-Aike Province is dominated by voluminous ignimbritic plateaus, with granites, lava domes, minor intermediate lavas and epiclastic tuffs. Locally, this volcanic unit receives different names (Table 1). In the Deseado Massif the volcanic rocks are predominantly flat-lying and relatively undeformed. In contrast, the rocks in the Andean Cordillera have been variably deformed, thrust and faulted during the Andean orogenic cycle.

The Serie Tobífera is widespread in the Austral, Malvinas and San Julián basins (Fig. 1), sparse outcrops are also found in the Ultima Esperanza region in Chile and Tierra del Fuego and the Isla de los Estados in Argentina. The Austral or Magallanes Basin extends over 170 000 km² in southernmost Argentina and Chile. NNW–SSE trending, it is limited by the Deseado Massif in the north, the Andean Fold and Thrust Belt in the west and the Río Chico Ridge in the east. Overlying a Palaeozoic metamorphic basement, the basin infill consists of a Jurassic rift silicic volcanoclastic sequence, Cretaceous sag-marine sediments and Tertiary foredeep shallow marine and conti-

mental deposits. In the proto-Pacific margin this unit is predominantly composed of subaqueous pyroclastic rocks, closely associated with turbiditic layers and polyimictic debris-flow deposits. Voluminous peperite breccias and hyaloclastites record the intrusion and quenching of rhyolitic magmas into wet sediments in a marine environment (Hanson and Wilson, 1993). Further east, the lithological composition of the Serie Tobífera is similar to the rest of the Chon-Aike Province, including subaerial rhyolitic lava flows and domes, epiclastics and pyroclastic flows. In the San Julián Basin 1385 m of rhyolites and rhyolitic tuffs have been drilled and in the western Austral Basin, a volcanoclastic assemblage of 2000 m thick has been reported (Figueiredo et al., 1996). In the easternmost Austral Basin and western Malvinas Basin, Galeazzi (1998) described the Dogger–Malm megasequence as a volcanic infill of half-grabens composed of tuffs, tuffaceous sandstones, rhyolites and minor black lacustrine sediments. The megasequence has been divided in two sequences, the 1500-m-thick ‘Lower Tobífera’ and the unconformably lying 500-m-thick ‘Upper Tobífera’ (Biddle et al., 1986; Galeazzi, 1998). The lower volcanoclastic sequence fills the deepest troughs and is absent over basement highs, whereas the upper Tobífera is a moderately continuous, easternwards wedging pyroclastic sequence which include dinoflagellates-bearing marine shales. In Tierra del Fuego, the equivalent Lemaire Formation, up to 1000 m thick, has been divided into four sequences consisting of epiclastic tuffs, dacitic and rhyolitic vitric tuffs and deep organic-rich lacustrine shales, which are considered to be a potential source for the hydrocarbons trapped in the area (Cagnolatti et al., 1996).

Table 1
Different stratigraphic names for the jurassic volcanoclastic unit in the South Chon-Aike Province

Deseado Massif	Austral, Malvinas and San Julian Patagonian Cordillera basins	
Bahía Laura Group: Chon-Aike Formation (large volume rhyolitic ignimbrites, tuffs, lava flows and domes) + La Matilde Formation (epiclastic, mostly lacustrine deposits and minor ignimbrites)	Serie Tobífera (large volume rhyolitic ignimbrites, tuffs, lava flows and domes, epiclastic deposits, peperites)	El Quemado Complex, Lemaire Formation (Argentina) = Ibañez Formation (Chile) (rhyolitic ignimbrites and lava flows, andesitic lavas and interbedded epiclastic tuffs, and peperites at the westernmost side)

3. Focus of study

Nine cores, from Cerro Norte, Campo Bremen and Océano Fields, located in the southeastern Austral Basin (Fig. 1), have been studied integrating petrographic and petrophysic techniques. Megascopic observation together with thin section studies in resin-impregnated selected samples were carried out in order to assess the different types of pore space. Porosity was measured in a constant volume cell employing a He porosimeter. Porosity and permeability was measured in 30-cm sampling intervals.

3.1. Cerro Norte field

This gas producing field is located on a structural high. Four wells have been drilled in homogeneous rhyolites, up to 150 m in thickness, which may be correlated all along the area.

In two studied cores from ACN-21 and ACN-28 wells the Serie Tobífera is represented by massive, yellowish grey to greenish white rhyolitic lavas with hydrothermal alteration. The ACN-21 core displays several oblique fractures with related mineralisation and hydraulic brecciation (Fig. 2A, 1698–1700 m). They are partially to completely filled by calcite, pyrite, Fe-oxides and clays (illite/smectite and kaolinite). The ACN-28 core exhibits autobrecciation (Fig. 2B, 1728.5–1730.5 m and 1732.2–1734 m). The irregularly shaped rhyolitic fragments, ranging from 10 to 50 cm in size, are immersed in a rhyolitic matrix. The fractures and microfractures follow a polyhedral pattern. Hydrothermal alteration is also pervasive, with calcite, chlorite and clays (illite/smectite and kaolinite) as the main fracture filling mineral phases.

The rhyolites show a porphyritic texture and carry 30–40% of phenocrysts including quartz, K-feldspar, scarce biotite and opaque minerals. The groundmass is completely recrystallised to a felsitic to granophyric aggregate. A remarkable feature is the presence of sieve texture in K-feldspar phenocrysts, which grades from hardly sieved crystals to relict sections. A newly formed K-enriched feldspar, optically discontinuous with the older one, rims the crystal cavities.

The rhyolites show a combination of 13–28% in

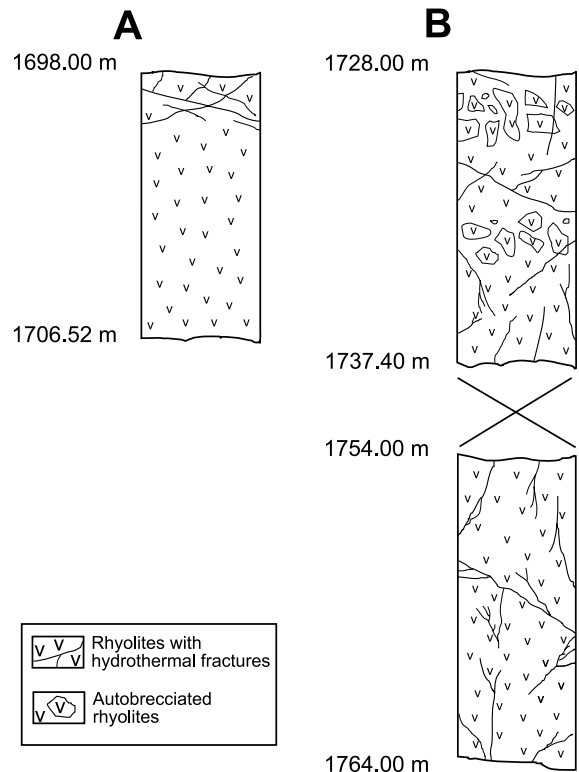


Fig. 2. Schematic section of Cerro Norte Field cores. (A) ACN-21. (B) ACN-28.

porosity and 0.001–6.7 mD in permeability (Fig. 3), remarkably uniform along vertical section. Three types of porosity may be distinguished: (1) intracrystalline porosity corresponding to K-feldspar sieve texture (Fig. 4A); (2) microfractures developed along the clast boundaries by autobrecciation (Fig. 4B); and (3) microfractures associated with hydrothermal processes.

3.2. Campo Bremen field

Three wells have been drilled in this gas producing field developed on a structural high, C-Bre-x2, ACBre-8 and ACBre-10. The Serie Tobífera is represented mainly by ignimbrites and minor interbedded epiclastic deposits. The Campo Bremen ignimbrites are moderately welded to non-welded and vertically zoned. Vapour-phase crystallisation zones and associated gas pipes are common. The composition is rhyolitic (quartz, K-

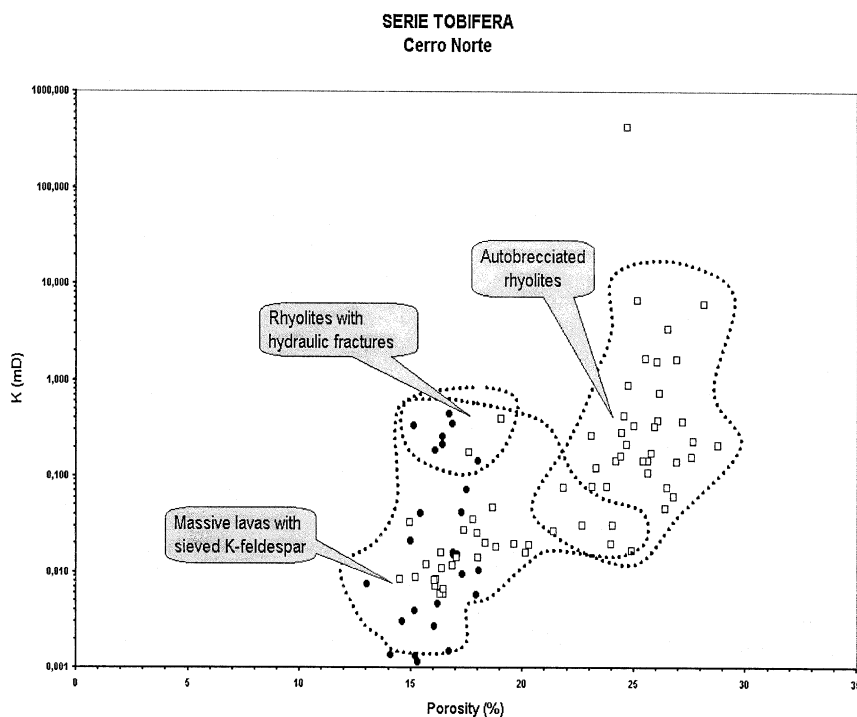


Fig. 3. Porosity vs. permeability (in mD) diagram for Cerro Norte Field. Symbols: filled circles, ACN-21; open squares, ACN-28. Three fields are defined considering the lithology and the processes involved.

feldspar, plagioclase, biotite, opaque minerals); these vitric tuffs are enriched in vitroclasts and depleted in lithic fragments. They usually show pervasive hydrothermal alteration with an assemblage consisting on chlorite, calcite, clays and quartz and associated hydraulic brecciation.

In CBre-x2 a 1.80-m-thick epiclastic deposit overlies the non-welded ignimbrites (Fig. 5A, 1775.20–1777 m). It consists of lithic conglomerates with sandstone matrix and calcite cement with interbedded laminated tuffites and lapillitic tuffs. The ignimbritic deposit shows a crude zonation due to well-developed eutaxitic intervals (Fig. 5A, 1778.3–1778.8 m and 1783.8–1785.3 m). A few mineralised fractures with pyrite and silica cut the core vertically.

In ACBre-8 the greenish grey ignimbrites, due to patchy chlorite impregnation, show slight vertical textural zonation. Variable in size (up to 3 cm), most of the pumices are undeformed and partially to completely altered to clay. Locally, fiammes occur. Lithic content is low: rhyolites,

andesites and older ignimbrites are randomly distributed. Gas pipes can be recognised as vertical to oblique open fissures, a few centimeters long and variably sinuous in shape (Fig. 5B, 1711.3–1713.2 m and 1727.00–1729.3 m). They usually show the best development in coincidence with the non-welded zones. In the deepest levels there is a crude zonation due to the presence of silicified intervals (Fig. 5B, 1731.6–1733.4 m). Also, several centimeter-long clay and silica filled fractures of hydrothermal origin are observed.

The ACBre-10 core is highly brecciated and displays oblique to subvertical fractures (Fig. 5C, 1722–1724.8 m) related to hydrothermal alteration, similar to ACBre-8. Welding increases gradually from a low degree zone in the upper part to a zone of remarkable eutaxitic texture at the bottom of the core (Fig. 5C, 1759.5–1759.9 m).

The ignimbrites contain 60–70% of vitroclasts, including pumice fragments and vitric shards. An assemblage of quartz, sieved K-feldspar, plagioclase and scarce biotite is included in a devitrified

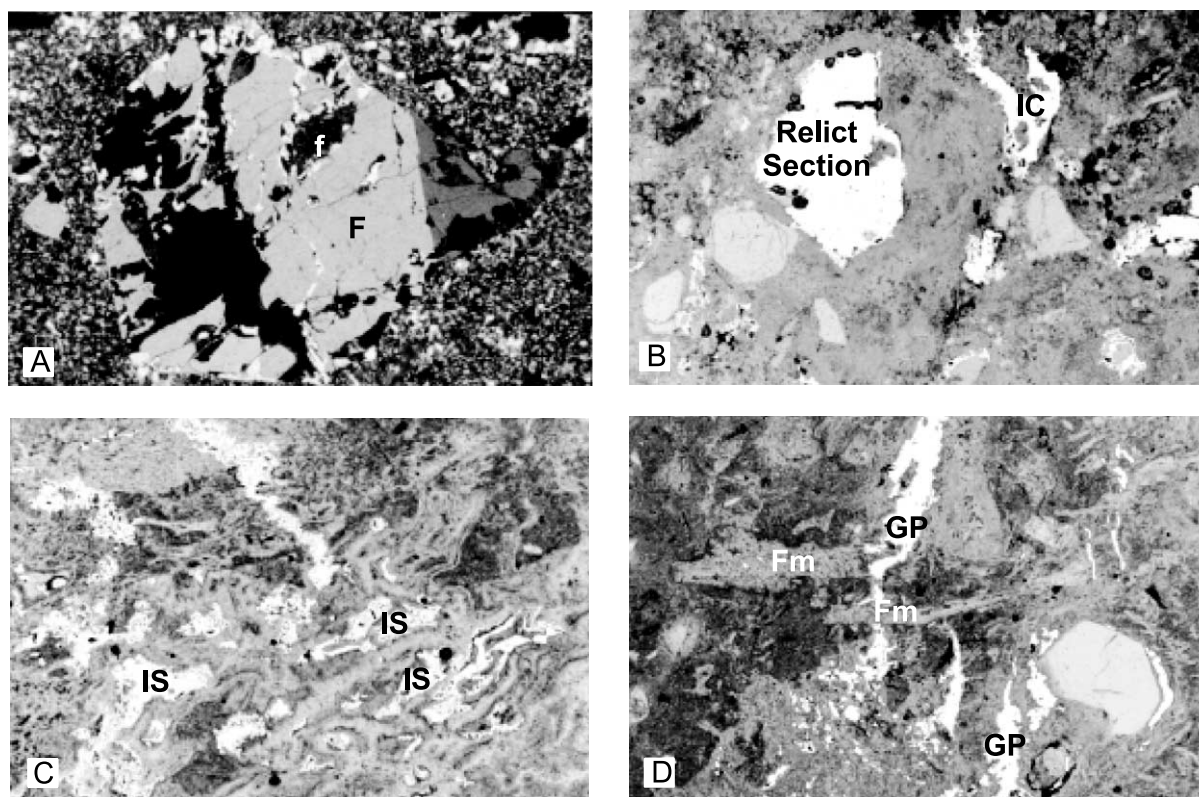


Fig. 4. Resin impregnated (in white) microphotographs. (A) Rhyolitic lava, late crystallised feldspar phase (f) rimming partially dissolved K-feldspar phenocryst (F), 2.5 \times . (B) Autobrecciated rhyolitic lava with feldspar relict section and interclast pore space (IC), 10 \times . (C) Ignimbrite with intershard porosity (IS), 5 \times . (D) Non-welded ignimbrite with gas pipes (GP) and connected fiammes (Fm), 2.5 \times .

groundmass with axiolitic, spherulitic and felsitic textures. Vitroclastic texture is dominant, however, eutaxitic texture may locally be observed. The zone of vapour-phase crystallisation is recognised by the presence of euhedral tiny crystals of quartz and K-feldspar. They grow in drusy habit along the borders of every available pore space as gas-pipes, microvesicles and relict phenocryst sections.

In these cores the porosity and permeability vary along the vertical section. The ignimbrites range between 4.8 and 26% in porosity and 0.002–164 mD in permeability (Fig. 6). The epiclastic rocks reach up to 22% in porosity and 200 mD in permeability.

Five types of porosity may be distinguished: (1) intershard porosity, which depends on the degree of welding (Fig. 4C); (2) gas pipe-related porosity

(Fig. 4D); (3) intracrystalline porosity corresponding to K-feldspar sieve texture; (4) microfractures associated to hydrothermal processes; and (5) intergranular porosity in the epiclastic rocks.

3.3. *Océano field*

Four wells, O-39, O-40, O-42 and O-43, have been drilled in this oil producing field which corresponds to a structural high. The Serie Tobífera is represented by different lithologies including vitrophyre, obsidian, hyaloclastite, ignimbrite and epiclastic breccia.

The vitrophyre (Fig. 7A, 1360–1367 m; Fig. 7C,D, the whole core) is yellowish and greenish to reddish coloured. It exhibits zones of massive perlitic glass and others with spherulitic and fel-

sitic textures. Locally, pseudoflow-banding texture is observed. Vitric material is moderate to highly altered to smectite, illite, clinoptilolite, erionite, quartz, opal and chlorite, resulting occasionally in a pseudoclastic texture. Alteration products also appear as infilling of open spaces as dissolution cavities, vesicles, perlitic cracks, quench and tectonic fractures and rarely as crystal replacement. Calcite in clusters and veins is rare. Crystal content is high (up to 40%) including plagioclase, sanidine, quartz and biotite; minor lithic fragments are also recognised. Frequently, shattered crystals are observed.

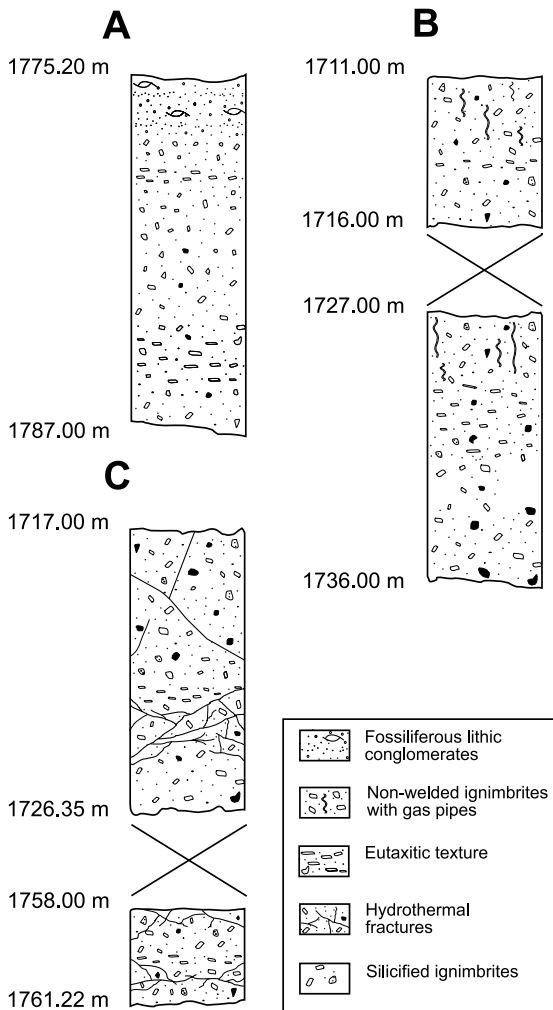


Fig. 5. Schematic section of Bremen Cores. (A) ACBre-x2. (B) ACBre-8; ACBre-10.

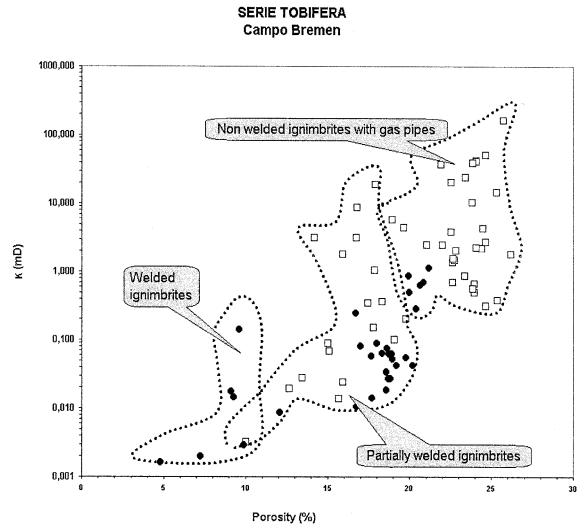
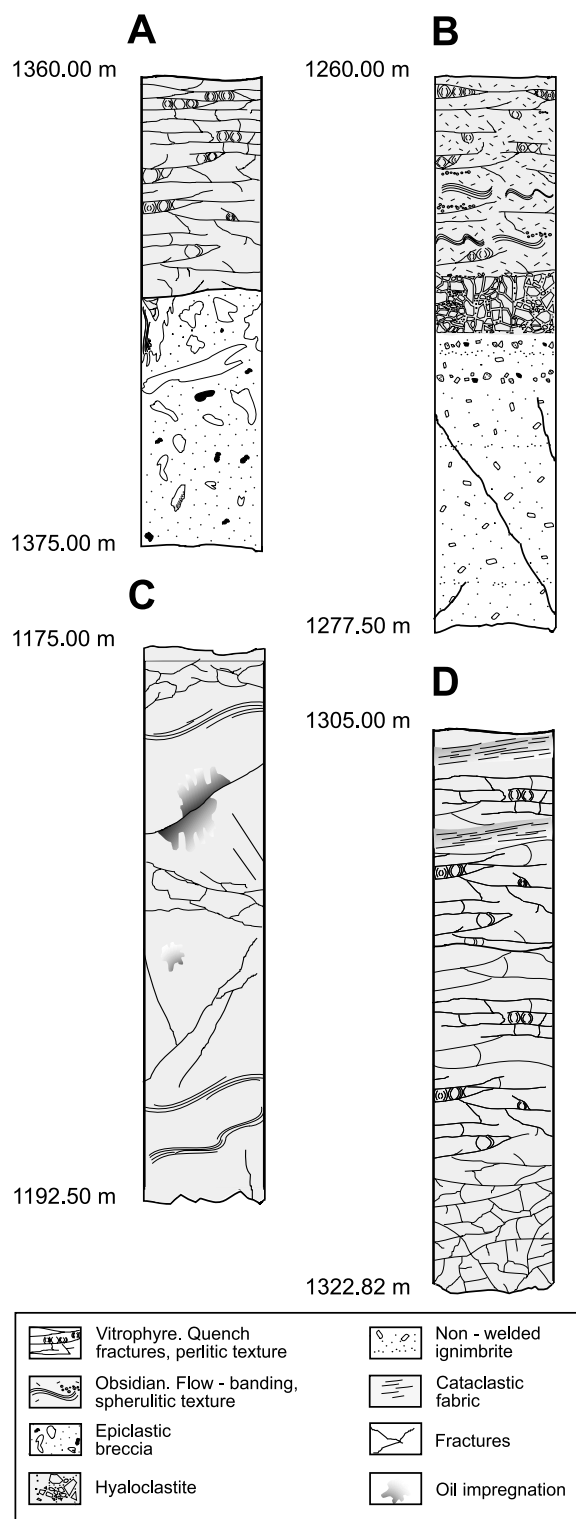


Fig. 6. Porosity vs. permeability (in mD) diagram for Bremen Field. Symbols: filled circles, ACBre-10; open squares, ACBre-8. Three fields are defined considering the lithology and the processes involved. Epiclastic rocks are not included.

The most remarkable feature in massive vitrophyres is the polyhedral curvilinear fracture pattern which results in a jigsaw-puzzle texture (Fig. 7A, 1360–1367 m; Fig. 7C,D, the whole core). These quench fractures are connected in an extended network. Perlitic texture is also very common, with perlites enclosed by the quench microfractures indicating that glass hydration occurred after quenching. Quench fractures and perlitic cracks are enlarged by glass dissolution which also generates open spaces heterogeneously distributed in the matrix. There are zones with hydrocarbon impregnation (Fig. 7C, 1178.7–1171.3 m and 1184–1185 m). In the upper part of the O-43 core a typically cataclastic fabric, indicating tectonic deformation, is observed. It is represented by sectors of dense displaced fractures and cataclastic zones that produce a crude shape-fabric (Fig. 7D, 1305–1306.2 m). Breakage, bending, displacement and deformation of the glass and crystals are conspicuous and typically cataclastic textures such as mica fish, tails and domino textures are displayed.

The obsidian (Fig. 7B, 1260–1266.2 m) is variably replaced by smectites, sericite, silica, clinop-



tilolite and minor chlorite. Although glass alteration is significant, primary volcanic features, such as parallel and convolute flow banding (Fig. 7B, 1263.5–1264 m and 1265–1265.4 m), spherulites, nodules, perlitic cracks and quench fractures are preserved. Perlitic cracks enclosed by quench fractures are clearly visible in some less altered sectors. Volcanic glass represents almost 95%, ranging from greenish black fresh perlitic and partially devitrified glass to almost completely yellowish grey to orange altered glass. Devitrification generates spherulitic, fan and bow/tie textures. Glass dissolution along quench and perlitic fractures is also frequent. Crystal content is low (up to 2%) and includes plagioclase and minor quartz. Shattered crystals are common.

The underlying hyaloclastite (Fig. 7B, 1266–1268 m), looks like a highly altered vitric breccia, reddish yellow and greenish grey in colour. Features indicating in situ fragmentation, such as jigsaw-puzzle texture, quench fractures, crystal shattering and gradation in clast size (Mc Phie et al., 1993), are clearly recognised. The breccia is monomict, composed by angular to subangular variably vesiculated vitric clasts. Perlitic obsidian fragments are dominant whereas pumice are subordinated. Ranging in size between lapilli and block (4–5 cm), they are immersed in a partially devitrified ash matrix. Devitrification is represented by spherulitic, microfelsitic and axiolitic textures. Broken plagioclase and quartz crystals are common. Smectite, silica and clinoptilolite are the main alteration products, occurring either as pervasive glass replacement or completely filling fractures.

The ignimbrite is an orange greyish massive lapillitic tuff, with some lapillitic layers in the upper part of the interval. This unit is cut by fractures filled with alteration products. White and orange unflattened pumice, partially replaced by clay and clinoptilolite are abundant. Along the unit the degree of welding is relatively low. Although lithic content is low, layers of lapillitic flow banded glass, old ignimbrites and rare

Fig. 7. Schematic section of Océano cores. (A) O-39. (B) O-40. (C) O-42. (D) O-43.

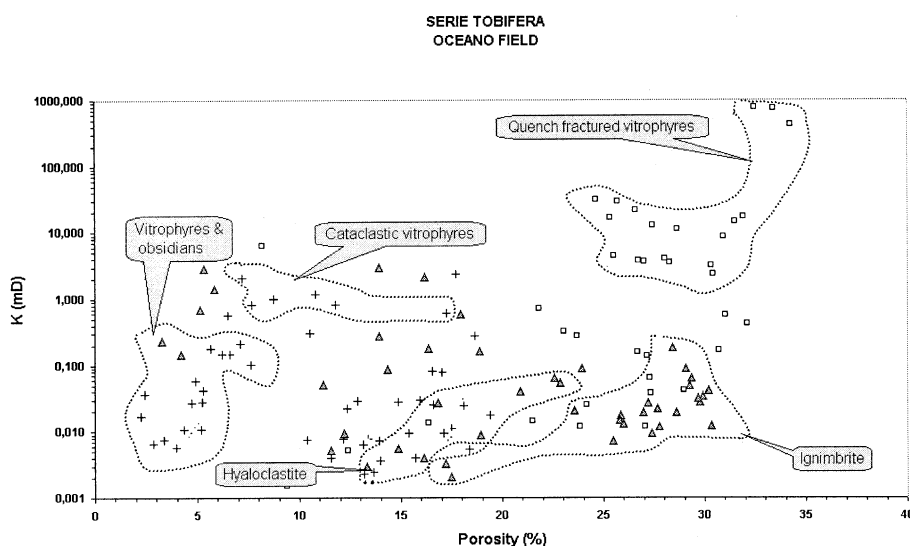


Fig. 8. Porosity vs. permeability diagram (in mD) for Océano Field. Symbols: open squares, O-39; filled triangles, O-40; crosses, O-43. The epiclastic breccia corresponds to all the open squares not included in the Quenched vitrophyres field. Samples which do not plot in the selected fields represent intermediate cases.

quartzite fragments are detected in the upper part of the ignimbritic unit (Fig. 7B, i.e. 1268.2–1268.8 m and 1269.2–1269.7 m). The abundant ash matrix includes a large number of blocky shards which are partially replaced by clinoptilolite. Crystal content is low (up to 10%), mainly plagioclase, quartz and scarce biotite.

The upwards coarsening epiclastic breccia (Fig. 7A, 1367–1375 m), includes different types of pyroclastic rocks, up to 1.5 m in size. Most of the clasts correspond to a white greenish chloritised very fine tuff, with some disconnected microfissures with dissolution halos. It has vitroclastic textures with the individual blocky type shards commonly replaced by chlorite. The morphology of the clasts, particularly their highly sinuous and interpenetrated contacts, indicate a plastic behaviour during deposition. Laminated organic-rich lapillitic tuff fragments, interpreted as pyroclastic surges (Fig. 7A, 1367–1369 m) are occasionally observed. Downward the size of the clasts decreases substantially and the breccia becomes matrix supported. Vitric lithoclasts of a different source, such as fresh perlitic glass, devitrified glass, pumices, porphyritic rhyolites and vitrophyres, are abundant. The matrix corresponds

to a cryptocrystalline aggregate with Fe-oxides impregnation.

Porosity and permeability are highly variable. Quenched glasses (vitrophyre and obsidian) achieve excellent porosity and permeability (up to 37.6% and 762 mD), except for the hyaloclastite which has low permeability (0.003–0.18 mD). The epiclastic breccia shows high variability in porosity (9.4–32%) and permeability (0.002–6.4 mD), but generally < 1 mD). The ignimbrites exhibit 17–30% in porosity and low permeability (< 0.1 mD) (Fig. 8).

Five types of porosity may be recognised: (1) quenching-related porosity, in dense glasses (Fig. 9A); (2) ubiquitous glass dissolution-related porosity (Fig. 9B); (3) intershard porosity, in non-welded to poorly welded ignimbrites; (4) secondary porosity, generated by tectonic deformation; and (5) intergranular porosity in the epiclastic breccia.

4. Porosity and permeability controls

Several processes take place after the volcanic rocks were emplaced on the surface and little is

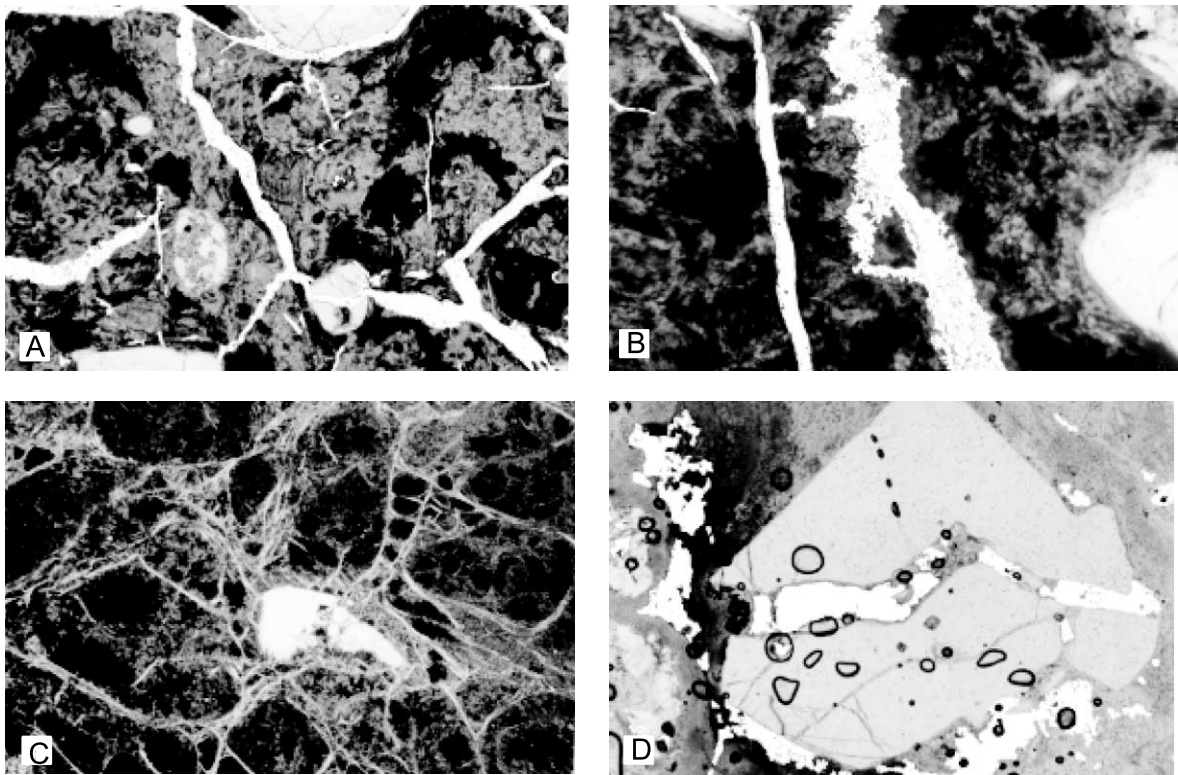


Fig. 9. Resin impregnated (in white) microphotographs. (A) Hyaloclastic vitrophyre with quench fractures, 2.5 \times . (B) Quench fractures enlarged by glass dissolution in hyaloclastic vitrophyre, 10 \times . (C) Perlitic cracks and quench fractures filled by smectites 2.5 \times . (D) Pore space in broken crystal, 2.5 \times .

known about how they modify their porosity and permeability. Unlike the lavas, which rapidly cooled upon emplacement, the ignimbritic flows are characterised by a protracted cooling history due to their extraordinary heat retention capacity.

They go through two stages: (1) the *pre-emplacment stage*, which includes vesiculation and fragmentation; and (2) the *post-emplacment stage* which embraces the cooling and post-cooling history (Table 2).

Table 2
Sequence of processes occurring during the volcanic stages

Stage	Processes
Pre-emplacment	Vesiculation Fragmentation
Post-emplacment	Cooling history <ul style="list-style-type: none"> Welding Devitrification Feldspar alteration Silicification Vapour-phase crystallisation Quench fragmentation and glass alteration
	Post-cooling history <ul style="list-style-type: none"> Hydrothermal alteration Weathering Tectonic deformation

In the pyroclastic rocks vesiculation is the main process which controls the primary porosity and permeability. The vesiculated nature of the ignimbrites creates a pore space suitable for releasing the dispersed gas phase. The basic mechanism involved is bubble coalescence, a continuous process that eventually leads to disruption of the melt phase. The development of intershard porosity depends on vesicularity, bubble size distribution, time, pressure difference, and viscosity (Klug and Cashman, 1996). Pore space is also generated among the broken pieces as a result of the fragmentation of inclusion-filled phenocrysts during this process (Fig. 9D).

During the cooling history different processes affecting pyroclastic rocks and lavas can modify, sometimes substantially, their original petrophysical characteristics. At this stage welding is the first order control of the original porosity in pyroclastic rocks. In non-welded to moderately welded ignimbritic deposits the pore space corresponds to former bubbles, gas pockets, non-flattened pumice fragments and loose packing of vitric shards (Fig. 4C). Progressive welding reduces porosity. However, due to the disconnection of the pore system, even in non-welded rocks, primary permeability is usually low. Porosity decreases dramatically due to welding, while permeability is always low, as can be seen in the studied cores of the Campo Bremen Field (Fig. 6).

Several deuteric processes during the early cooling history, such as feldspar alteration, silicification, and vapour-phase crystallisation, may change the original petrophysical parameters. The feldspar sieve texture, so commonly observed in both rhyolites and ignimbrites, is produced by dissolution of crystal phases by deuteric fluids. The best time constraint for feldspar dissolution is the presence of vapour phase crystals in relict sections and the precipitation of a newly formed K-feldspar (Fig. 4A). This sieve texture results in an intracrystalline porosity where the pores are rarely connected, therefore the permeability is always low, as can be seen in the rhyolites of Cerro Norte Field (Fig. 3). Ion microprobe studies have proven a primary porosity in feldspars produced by the presence of micropores roughly proportionally to the water content of the parent mag-

ma. These micropores generate a micropermeability that allow the fluids to penetrate into the grains leading to dissolution processes (David and Walker, 1990). Feldspar alteration involves an initial dissolution stage, usually non-stoichiometric in fluids with a low pH, followed by precipitation of secondary phases. However, in diluted solutions precipitation of secondary minerals does not necessarily occur (Blum and Stilling, 1995).

Deuteric silicification is widespread and ubiquitous and appears as a massive form of glass replacement. The development of a Vapour Phase Crystallisation Zone in ignimbritic deposits produces a significant increase of permeability due to the presence of gas pipes and interconnected perpendicular pumice fragments (Fig. 6) (Fig. 4D).

In rhyolitic lavas, autobrecciation is a cooling-history process which may enhance porosity and permeability, like in the Cerro Norte rhyolites (Fig. 3). Along the lava clasts boundaries, a pore space is developed due to the relatively loose packing of the rhyolitic fragments during brecciation. The pores are small but they may generate a connected network (Fig. 4B).

Magma–water interaction results in quench fragmentation and the formation of hyaloclastites (Mc Phie et al., 1993). Océano Field cores provide strong evidence for magma–water interaction: abundant glass, quench fractures affecting vitrophyres and obsidians, hyaloclastic deposits with jigsaw-puzzle texture and the presence of clinoptilolite in the alteration assemblage. The quench fractures system becomes a very well connected pore system (Figs. 8 and 9A). Closely associated perlitisation also improves the permeability. Water interaction also produces glass dissolution and alteration (Mc Phie et al., 1993). In Océano Field glasses, dissolution increases porosity and permeability (Fig. 9B) expanding open spaces of different origin whereas alteration only enhances porosity when coherent glass is replaced by micas and clay aggregates. Secondary mineral precipitation may partially to completely occlude the open spaces even sealing them (Fig. 9C), reducing dramatically porosity and permeability (Fig. 8). Equilibria between dissolution and precipitation depends on chemical conditions which are con-

trolled by the grade of glass-water interaction and the freshwater influx (de'Genaro et al., 2000). Those parameters depend on the relative location in the volcanic pile and the available water mass.

Among the post-cooling processes (Table 2), both hydrothermal alteration and tectonic deformation cause significant changes in the porosity and permeability. As a consequence of hydrothermal alteration, a hydraulic fracture network is locally developed. When the fractures and microfractures are sealed with mineralisation, they reduce the bulk permeability. Similarly, tectonic fractures and cataclastic zones contribute to enhance porosity and permeability (Fig. 8).

The diagram of Fig. 10 is an attempt of integrating different lithologies, processes and petrophysical data from all the studied cores. It shows that measured porosity and permeability in volcanic rocks is strongly dependent not only on the original petrophysical character but on the cooling and post-cooling processes as well.

Attending to the quality assessment of the Tobífera fluid reservoirs, the highest permeability corresponds to quench fractured glasses and non-welded ignimbrites with gas pipe structures, followed by autobrecciated rhyolites. The situation with the lowest porosity/permeability is repre-

sented by welded ignimbrites, massive glasses, and fresh rhyolites.

5. Conclusions

This study demonstrates that the petrophysical parameters of the Tobífera volcanic reservoirs are not only controlled by tectonic deformation but predominantly by processes inherent to the volcanic events. In fact, porosity and permeability are generated by a sequence of processes which span from the volcanics pre-emplacment history up to their post-cooling stage. These processes show relative significance in generating and modifying the petrophysical parameters. Their effects may be additive or one process may cancel the effect of the other. The application of these concepts together with suitable volcanological models may make Tobífera-like reservoirs better exploration targets for oil exploration.

Acknowledgements

We thank Shan de Silva and Maurizio de'Genaro for constructive reviews of the manuscript. We are grateful to J. Varekamp for his help in preparing the final edition, which led to a much improved version. We also thank Chevron San Jorge S.A. for allowing us to publish the petrophysical data.

References

- Biddle, K.T., Uliana, M.A., Mitchum, R.M. Jr., Fitzgerald, M.G., Wright, R.C., 1986. The stratigraphic and structural evolution of the central and eastern Magallanes Basin, southern South America. *Int. Assoc. Sedimentol. Spec. Publ.* 8, pp. 42–61.
- Blum, A.E., Stilling, L.L., 1995. Feldspar dissolution kinetics. In: White, Brantley (Eds.), *Chemical Weathering Rates of Silicate Minerals*. Reviews in Mineralogy 31.
- Cagnolatti, M.J., Martins, R., Villar, H.J., 1996. La Formación Lemaire como probable generadora de hidrocarburos en el área Angostura, provincia de Tierra del Fuego, Argentina. *13° Congreso Geológico Argentino y 3° Congreso de Exploración de Hidrocarburos*, vol. 1, pp. 123–139.
- Cazeneuve, H., 1965. Datación de una toba de la Formación

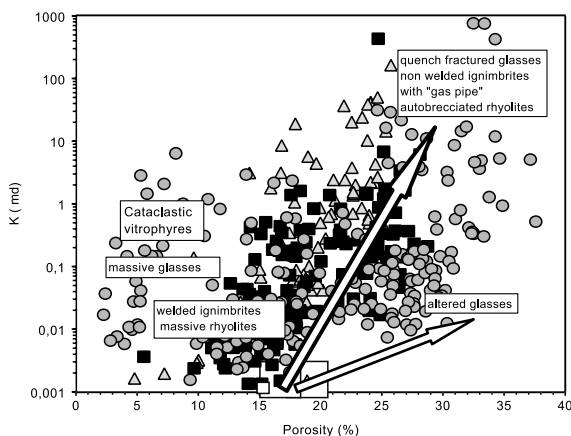


Fig. 10. Porosity vs. permeability diagram showing the main lithologies and processes studied in the Cerro Norte Field (filled squares), Campo Bremen Field (filled triangles) and Océano Field (filled circles). Increasing trends in porosity and permeability are shown by arrows.

- Chon-Aike (Jurásico de Santa Cruz), Patagonia. *Ameghiniana* 4, 156–158.
- David, F., Walker, L., 1990. Ion microprobe study of intra-grain micropermeability in alkali feldspars. *Contrib. Mineral. Petrol.* 139, 17–35.
- de'Genaro, M., Capelletti, P., Langella, A., Perrotta, A., Scarpatti, C., 2000. Genesis of zeolites in the Neapolitan Yellow Tuff: Geological, volcanological and mineralogical evidence. *Contrib. Mineral. Petrol.* 106, 124–128.
- Figueiredo, A.M.F., Pellón de Miranda, A., Ferreira, R.F., Zalan, P.V., 1996. Cuenca de San Julián. In: Ramos, V.A., Turic, M.A. (Eds.), 13° Congreso Geológico Argentino y 3° Congreso de Exploración de Hidrocarburos. *Geología y Recursos Naturales de la Plataforma Continental Argentina*, Relatorio 11, pp. 193–212.
- Galeazzi, J.S., 1998. Structural and stratigraphic evolution of the Western Malvinas Basin, Argentina. *Am. Assoc. Pet. Geol.* 82, 596–636.
- Hanson, R.E., Wilson, T.J., 1993. Large-scale rhyolite peperites (Jurassic, southern Chile). *J. Volcanol. Geotherm. Res.* 54, 247–264.
- Kay, S.M., Ramos, V.A., Mpodozis, C., Sruoga, P., 1989. Late Paleozoic to Jurassic silicic magmatism at the Gondwana margin: Analogy to the Middle Proterozoic in North America? *Geology* 17, 324–328.
- Klug, C., Cashman, K.V., 1996. Permeability development in vesiculating magmas: Implications for fragmentation. *Bull. Volcanol.* 58, 87–100.
- Mc Phie, J., Doyle, M., Allen, R., 1993. *Volcanic Textures. A Guide to the Interpretation of Textures in Volcanic Rocks.* University of Tasmania, Tasmania, 196 pp.
- Pankhurst, R.J., Leat, P.T., Sruoga, P., Rapela, C.W., Márquez, M., Storey, C., Riley, T.R., 1998. The Chon-Aike province of Patagonia and related rocks in West Antarctica: A silicic large igneous province. *J. Volcanol. Geotherm. Res.* 81, 113–136.
- Pankhurst, R.J., Riley, T.R., Fanning, C.M., Kelley, S.P., 2000. Episodic silicic volcanism in Patagonia and the Antarctic Peninsula: Chronology of magmatism associated with the break-up of Gondwana. *J. Petrol.* 41, 605–625.
- Ramos, V.A., 1996. Evolución tectónica de la Plataforma Continental. In: Ramos, V.A., Turic, M.A. (Eds.), 13° Congreso Geológico Argentino y 3° Congreso de Exploración de Hidrocarburos. *Geología y Recursos Naturales de la Plataforma Continental Argentina*, Relatorio 21, pp. 385–404.
- Schalamuck, I.B., de Barrio, R.E., Zubia, M.A., Genini, A., Echeveste, H., 1999. Provincia auroargentífera del Deseado, Santa Cruz. In: Zappettinni, E.O. (Ed.), *Recursos minerales de la República Argentina*, Buenos Aires, *Anales* 35, pp. 1177–1188.
- Sruoga, P., 1989. Estudio petrológico del plateau ignimbrítico jurásico a los 47° 30' L.S. Unpubl. Ph.D. Thesis, Universidad Nacional de La Plata, 400 pp.
- Sruoga, P., 1994. El Complejo Caldera La Peligrosa, Cordillera Patagónica Austral (47° 15' L.S.). *Actas del VII Congreso Geológico Chileno*, Concepción 2, 1219–1223.
- Storey, B.C., Alabaster, T., Hole, M.J., Pankhurst, R.J., Wever, H.E., 1992. Role of subduction – plate boundary forces during the initial stages of Gondwana break-up: Evidence from the Proto-Pacific margin of Antarctica. In: Storey, B.C., Alabaster, T., Pankhurst, R.J. (Eds.), *Magmatism and the Causes of Continental Break-up*. *Geol. Soc. Spec. Publ.* 68, pp. 149–164.